Realization of artificial Josephson topological materials via three-terminal proximity interferometers

Francesco Giazotto
NEST, Istituto Nanoscienze-CNR & Scuola Normale Superiore, Pisa, Italy

Exotic New States in Superconducting Devices: the Age of the Interface

Johannes Gutenberg Universität, Mainz
Germany, 25-28 September 2017

Outline

1. Motivations

2. AR and PE in hybrid SNS systems – impact on the density of states
   - Phase dependence of proximity-induced modification of the DOSs
   - Probing the proximized DOSs: experiments with STM spectroscopy

3. Superconducting quantum interference proximity transistor (SQUIPT)
   - Implementation
   - Experimental results and comparison with theory

4. A three-terminal double-loop Josephson interferometer: the ω-SQUIPT
   - Implementation
   - Structure fabrication details
   - Experimental results & comparison with theory
   - Topological classification
   - Properties of topological states
   - Robustness in temperature

5. Conclusions & future perspectives

Motivation: creation of *Josephson* topological materials

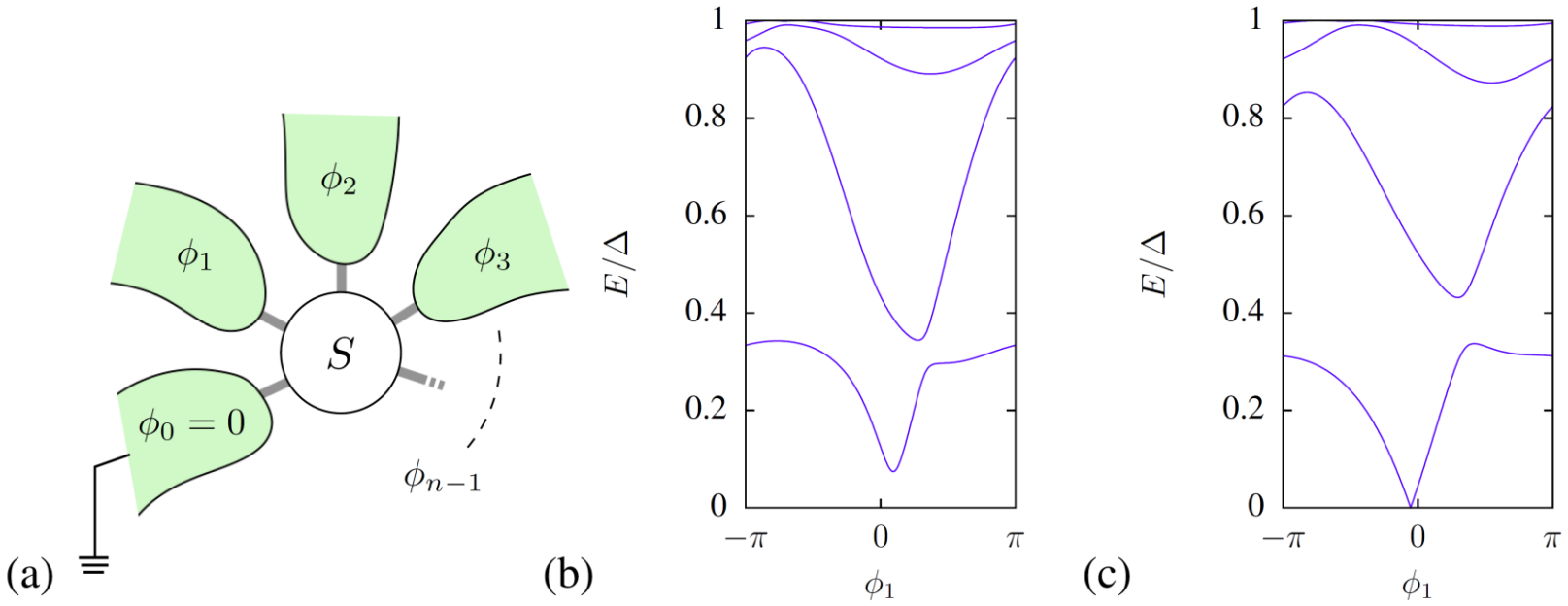

- R.-P. Riwar, M. Houzet, J. S. Meyer, Yu. V. Nazarov, *Multi-terminal Josephson junctions as topological materials,* Nat. Commun., 11167 (2016);
- C. Padurariu *et al*., PRB **92**, 205409 (2015);
- B. van Heck et al., PRB **90**, 155450 (2014);
- T. Yokoyama and Yu. V. Nazarov, PRB **92**, 155437 (2015)

- (N-1)-dimensional space of phases
- N = 3 + Spin orbit --> Majorana's like
- N = 4 --> Weyl singularities
- …..

Proximity effect & supercurrent

Metallic contact between a normal metal and a superconductor

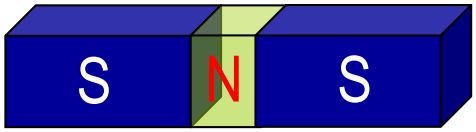

Electron-hole correlations: proximity effect

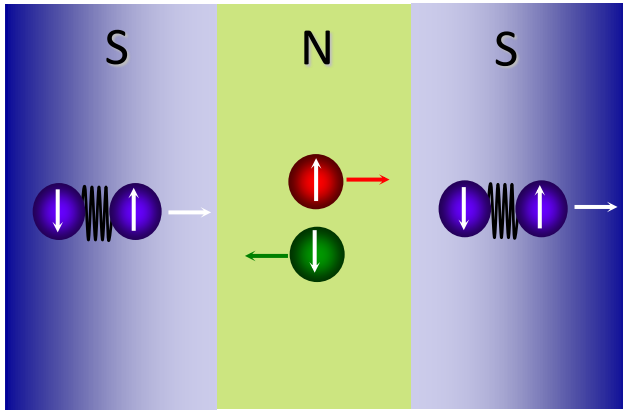

Andreev reflection

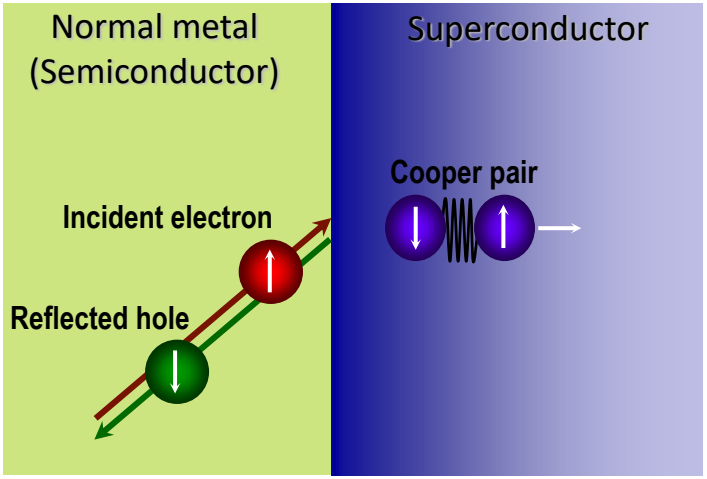

Supercurrent → Andreev bound states (ABS)

Proximity effect in SNS systems: basic formalism

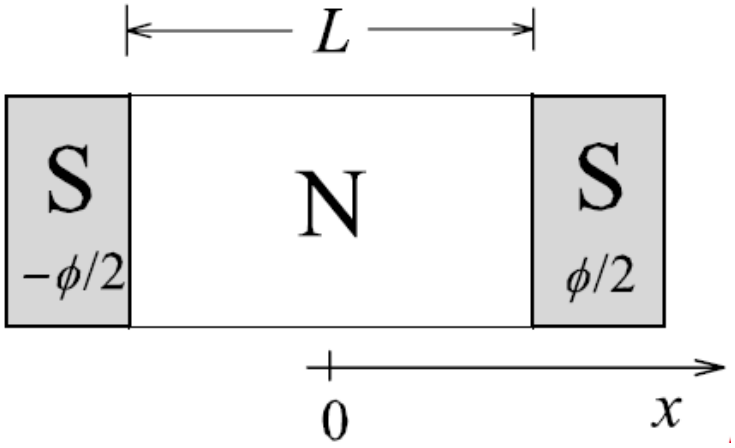

Diffusive mesoscopic N wire:

quasi-1D geometry

$L_\phi > L >> l_e$

D = diffusion coefficient

Δ = superconducting order parameter

ϕ = macroscopic phase of the order parameter

$E_{Th} = hD/2\pi L^2$ Thouless energy

Usadel equations

$$\hbar D\partial_x^2\theta = -2iE\sinh(\theta) + \frac{\hbar D}{2}(\partial_x\chi)^2\sinh(2\theta),$$

$$\sinh(2\theta)\partial_x\theta\partial_x\chi + \sinh^2(\theta)\partial_x^2\chi = 0$$

$$\theta(\pm L/2) = \operatorname{arctanh}(\Delta/E)$$

$$\chi(\pm L/2) = \pm\phi/2$$

LDOS

$$\mathcal{N}(x,E,T,\phi) = N_F\mathrm{Re}\{\cosh[\theta(x,E,T,\phi)]\}$$

LDOS properties:

$N(-E) = N(E)$

E_g for $|E| \leq E_g$

$E_g(\phi = 0) \approx 3.2E_{Th}$ for $\Delta >> E_{Th}$

$E_g(\phi = \pi) = 0$

Modification of the LDOSs in SNS junctions due to proximity effect

Length and position dependence

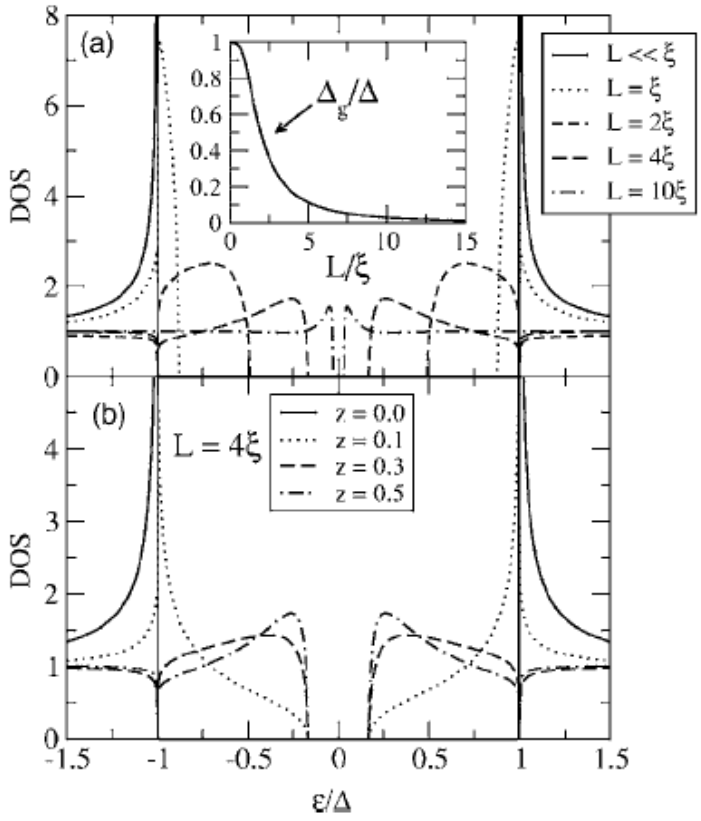

FIG. 1. (a) Normalized density of states in the middle of the wire (z=0.5) as a function of energy for different wire lengths. The inset shows the minigap Δ_g as a function of the length. (b) Normalized density of states as a function of the energy in different positions (z) along a wire of length L=4ξ.

J. C. Cuevas *et al.*, PRB **73**, 184505 (2006)

Phase dependence

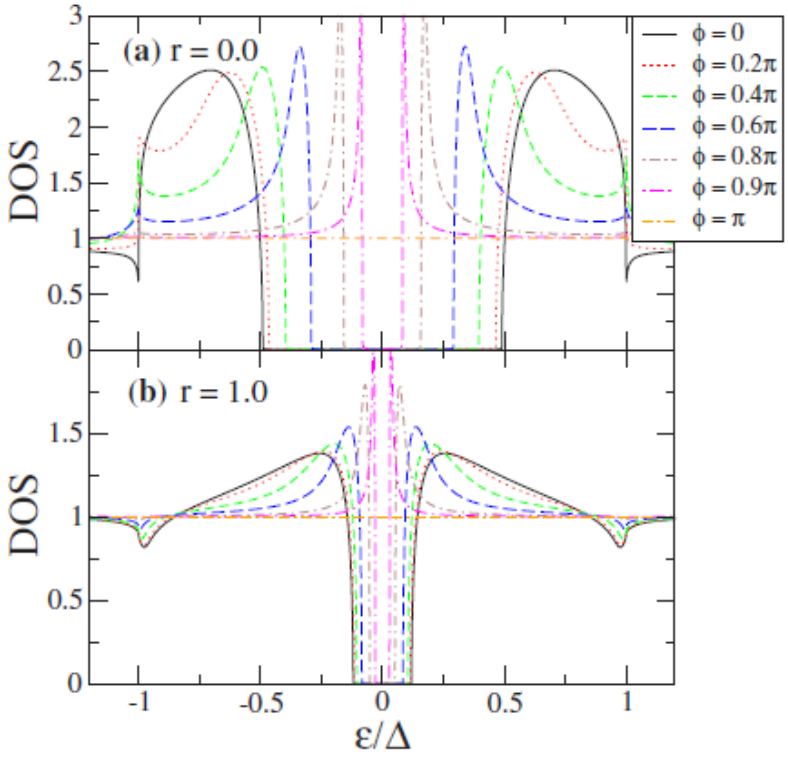

FIG. 3. (Color online) Density of states of a SNS junction as a function of energy in the middle of a wire of length L=2ξ (Γ_{sf} =0) for different values of the superconducting phase difference ϕ. The interfaces are identical and characterized by a ratio r=G_N/G_B=0.0 in panel (a) and r=1.0 in panel (b). In both cases, τ=1.

J. C. Hammer *et al.*, PRB **76**, 064514 (2007)

Phase-dependence of PE probed with STM spectroscopy (i)

PRL 100, 197002 (2008) PHYSICAL REVIEW LETTERS week ending 16 MAY 2008

Phase Controlled Superconducting Proximity Effect Probed by Tunneling Spectroscopy

H. le Sueur, P. Joyez, H. Pothier, C. Urbina, and D. Esteve
Quantronics group, Service de Physique de l'Etat Condensé (CNRS URA 2464), CEA-Saclay, 91191 Gif-sur-Yvette, France
(Received 31 January 2008; published 14 May 2008)

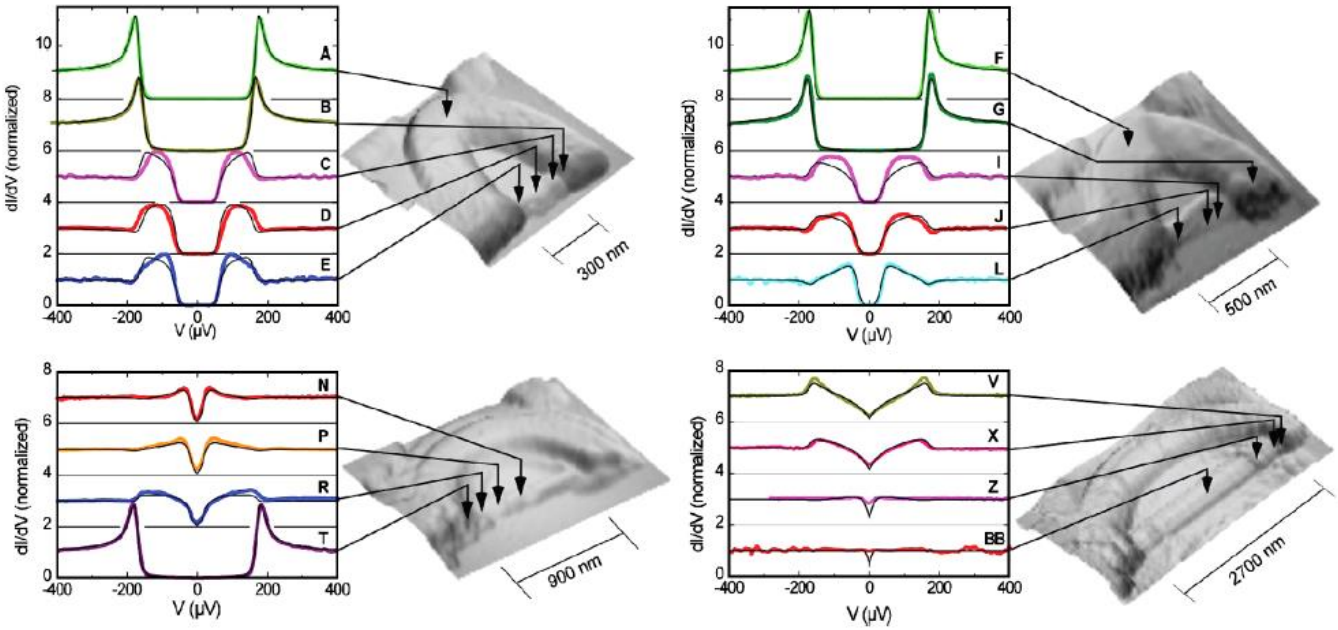

FIG. 2 (color online). Measured (thick lines) differential conductance taken for zero flux through the loop at various positions (indicated by the arrows and labeled by capital letters) of the four SNS structures shown by the AFM images (taken at 35 mK). The length of the silver wire is, respectively, (a) 300 nm, (b) 500 nm, (c) 900 nm, (d) 2700 nm. The curves are normalized to 1 at large voltage and are shifted by integer numbers for clarity. The thin black solid lines correspond to the model based on the quasiclassical theory of superconductivity introduced in the text and described more in depth in Ref. [15].

Al/Ag SNS proximity SQUIDs

Phase-dependence of PE probed with STM spectroscopy (ii)

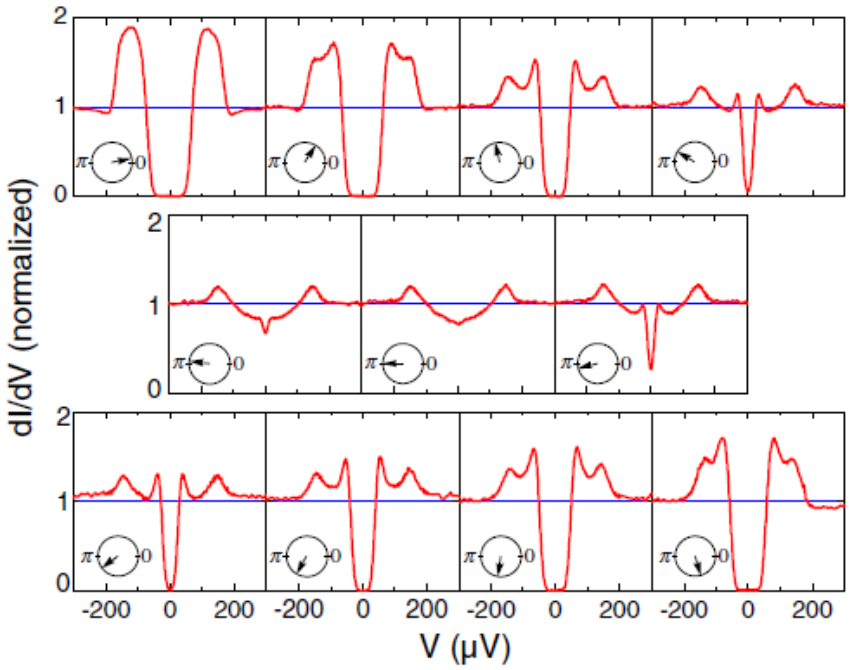

FIG. 3 (color online). Differential conductance $dI/dV(V)$ versus voltage measured in the middle of the 300 nm-long Ag wire (position D) for different values of the phase difference across it as shown by the phase clocks ($\varphi/\pi = 0.06,\ 0.32,\ 0.57,\ 0.83;\ 0.96,\ 1.00,\ 1.08;\ 1.21,\ 1.34,\ 1.46,\ 1.59$).

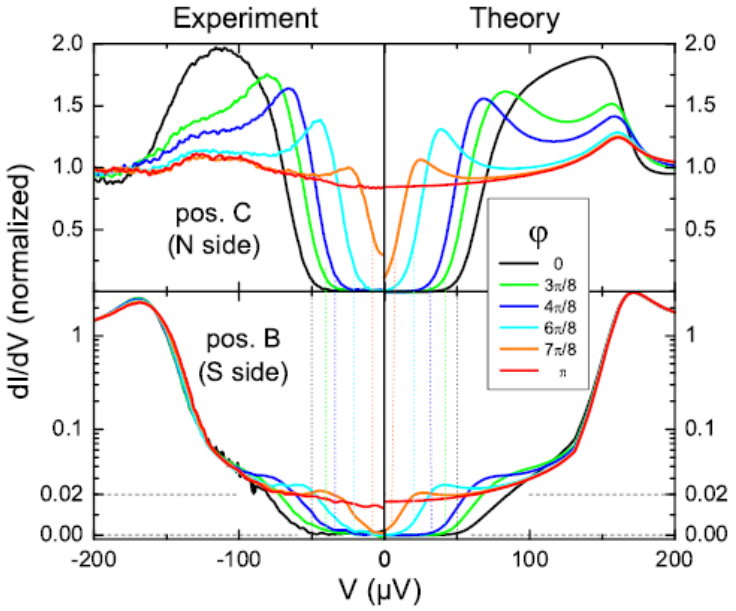

FIG. 4 (color online). Differential conductance versus voltage, for different values of the phase difference φ across the 300 nm-long Ag wire. Left quadrants: measured. Right quadrants: calculated. Top: on the N side (position C); Bottom: on the S side, close to the interface (position B: note that the scale is linear up to 0.02 and logarithmic above, to magnify the variation for small subgap conductance). This shows that the minigap is also present on the superconductor side with the same value as on the N side. Dashed lines are guides to the eye.

Phase-evolution of PE → Full phase-control of the minigap amplitude

Experiment to theory comparison

H. le Sueur *et al.*, PRL **100**, 197002 (2008)

The SQUIPT: a novel quantum interferometer

Active manipulation of the DOS of a proximity N metal

Phase control (through magnetic flux)

Detection (through tunnel junctions)

High sensitivity for flux detection

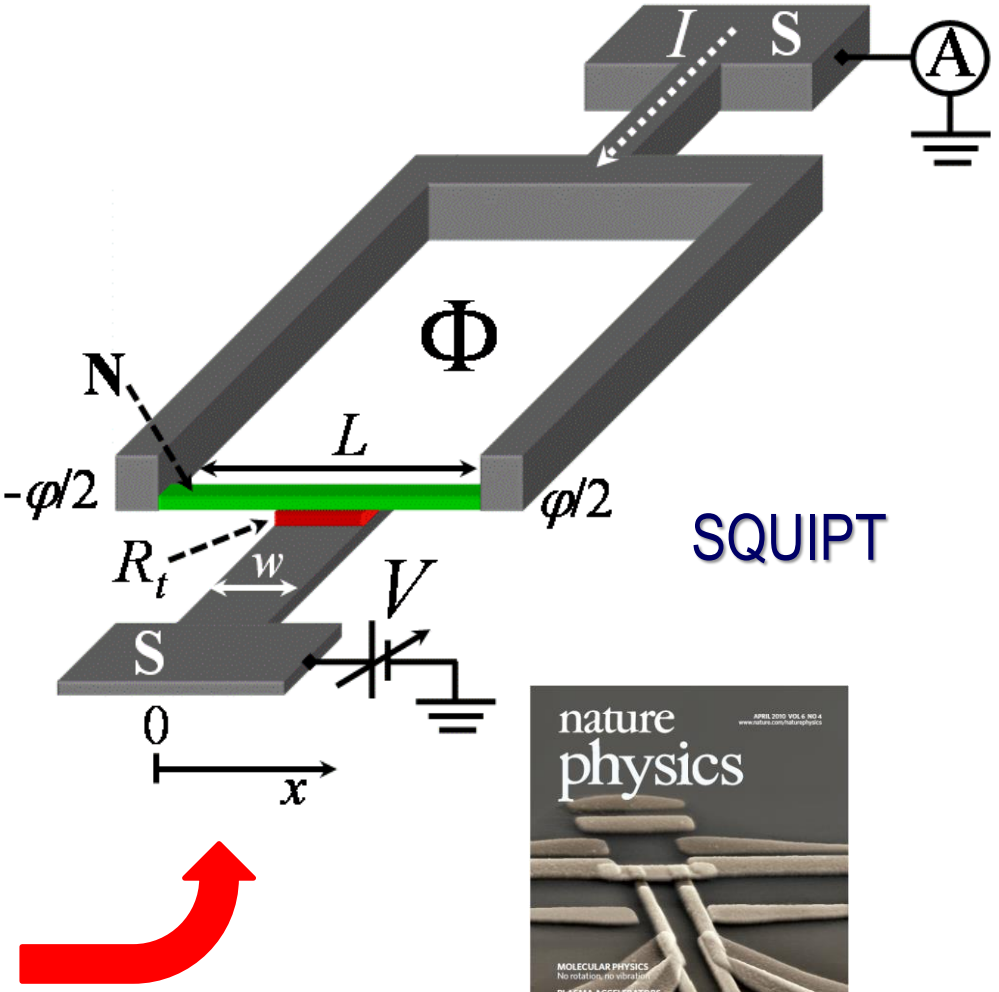

SQUIPT

FG *et al.*, Nat. Phys. **6**, 254 (2010);
M. Meschke et al., PRB **84**, 214514;
A. Ronzani et al., PRAppl. **2**, 024005 (2014);
S. D'Ambrosio et al., APL **107**, 113110 (2015)

SQUIPT: setups

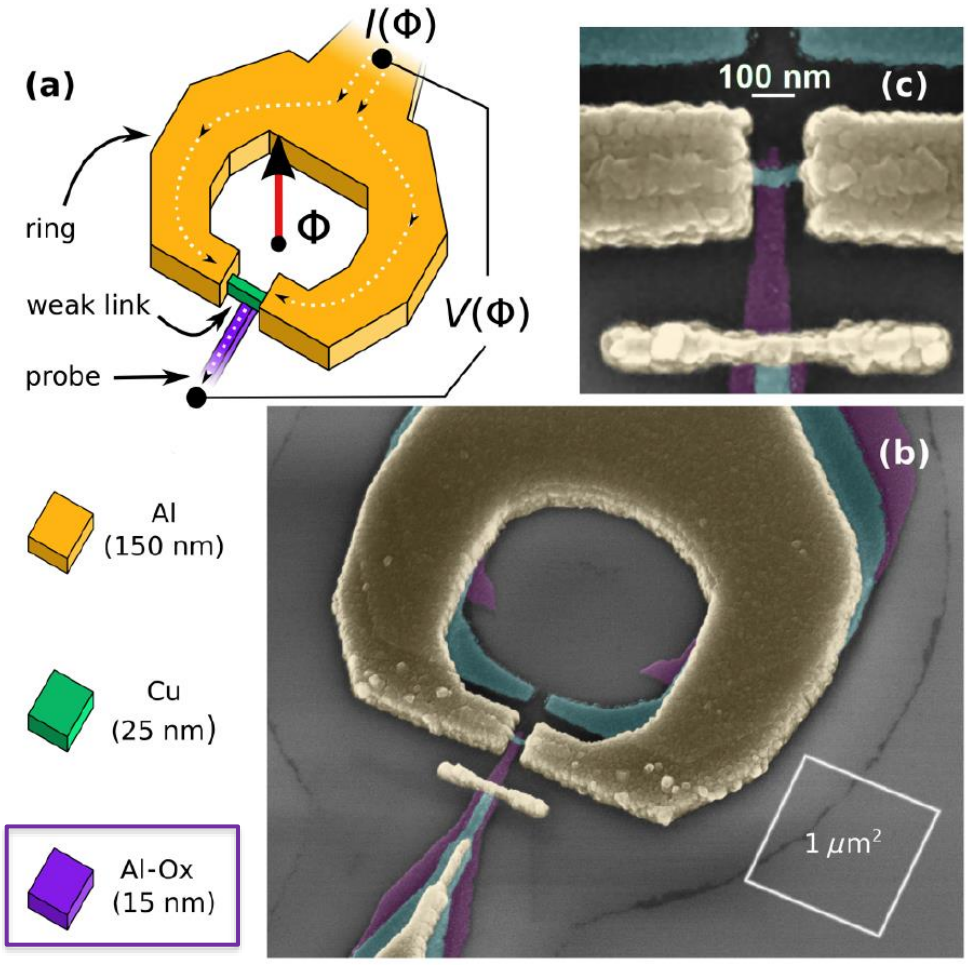

S probe

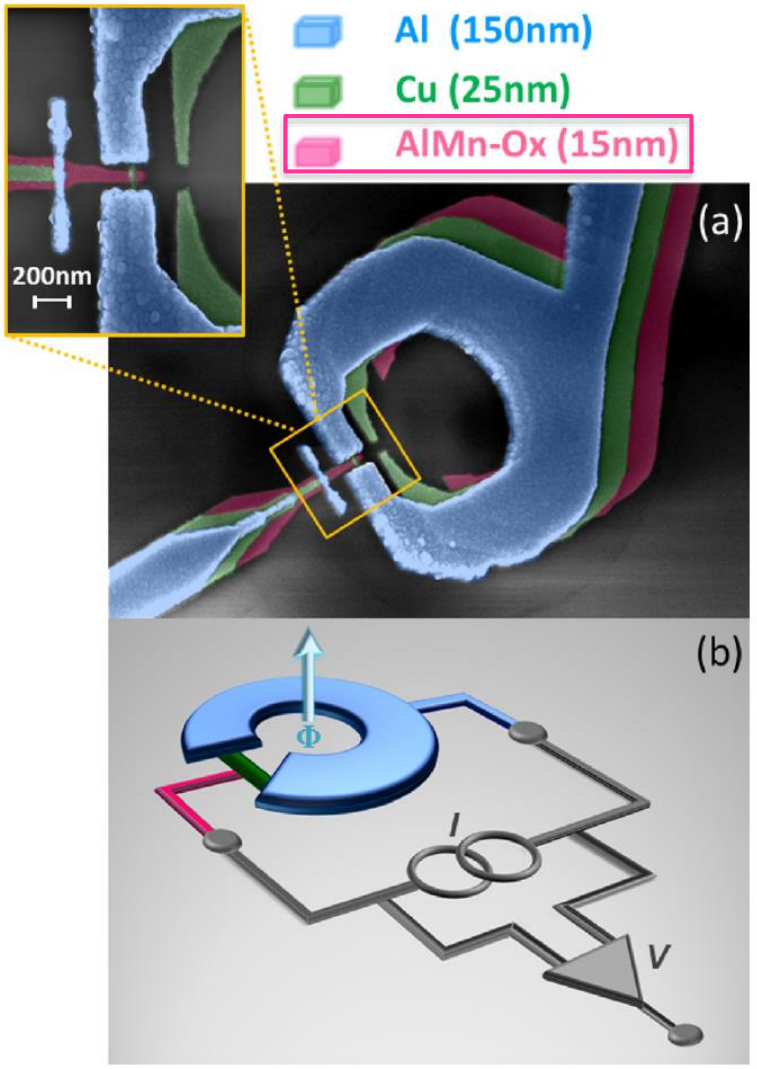

N probe

FG *et al.*, Nat. Phys. **6**, 254 (2010);
M. Meschke et al., PRB **84**, 214514 (2011);
A. Ronzani et al., PRAppl. **2**, 024005 (2014);
S. D'Ambrosio et al., APL **107**, 113110 (2015)

SQUIPT: behavior

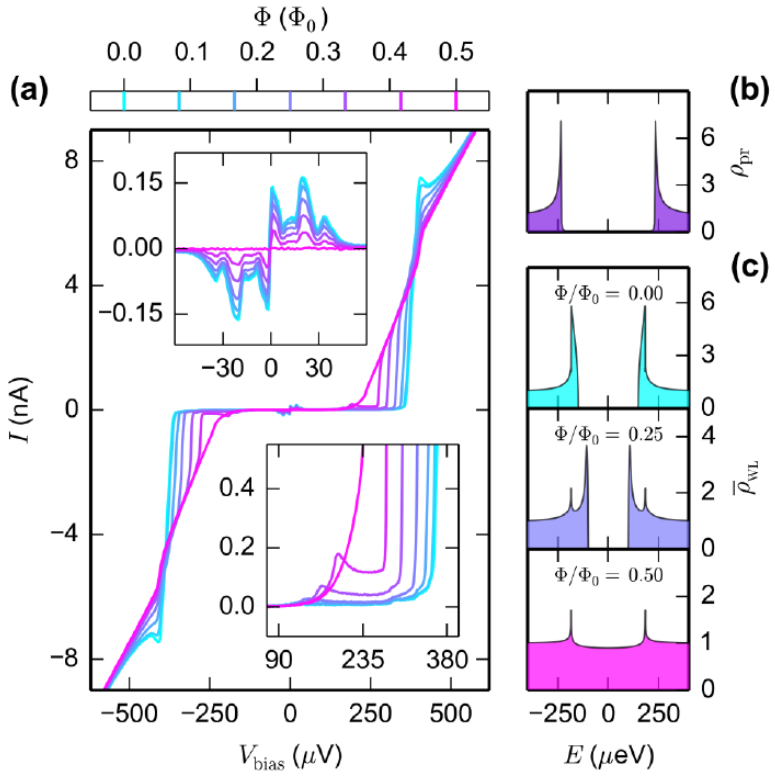

S probe

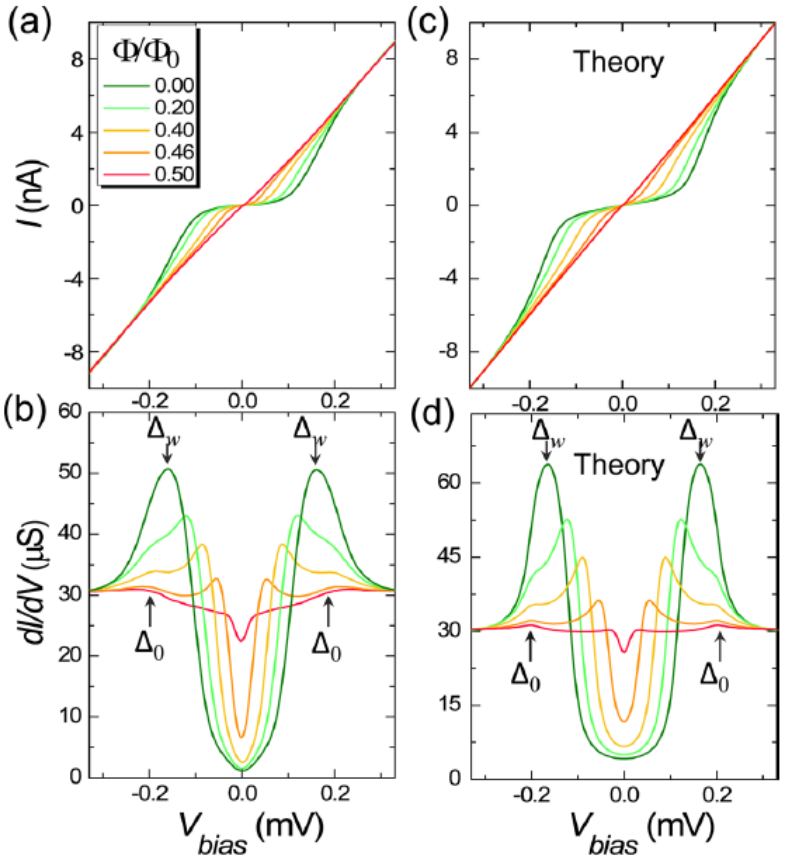

N probe

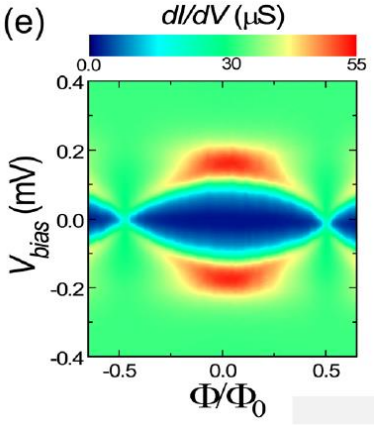

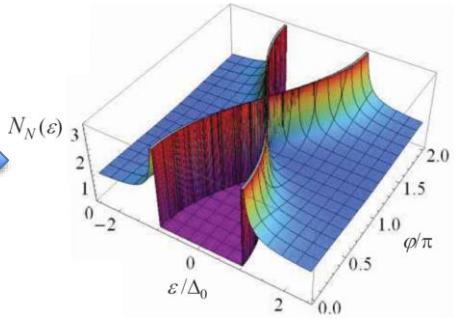

FG *et al.*, Nat. Phys. **6**, 254 (2010);
M. Meschke et al., PRB **84**, 214514 (2011);
A. Ronzani et al., PRAppl. **2**, 024005 (2014);
S. D'Ambrosio et al., APL **107**, 113110 (2015)

SQUIPT: performance

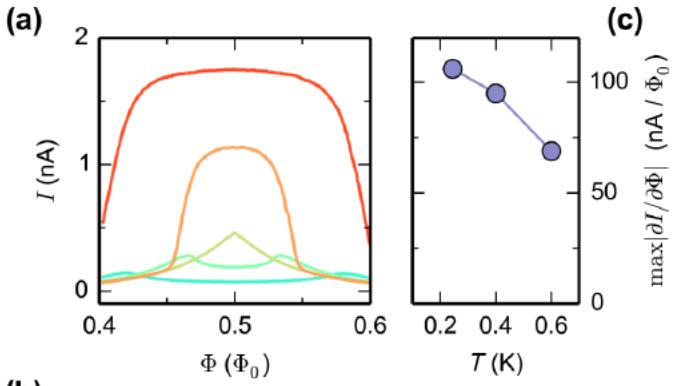

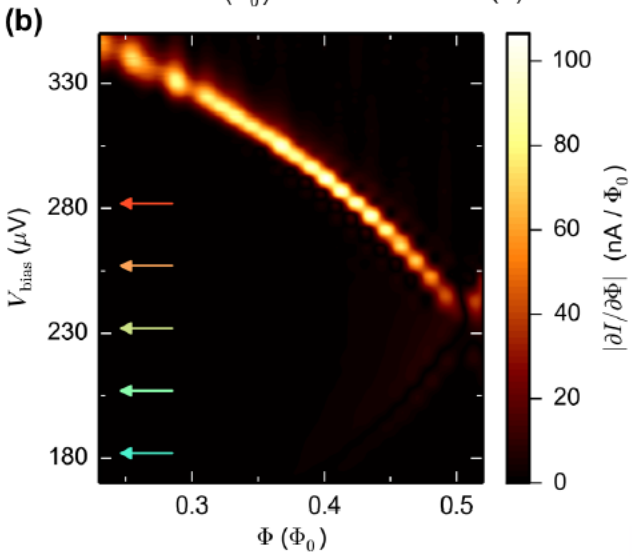

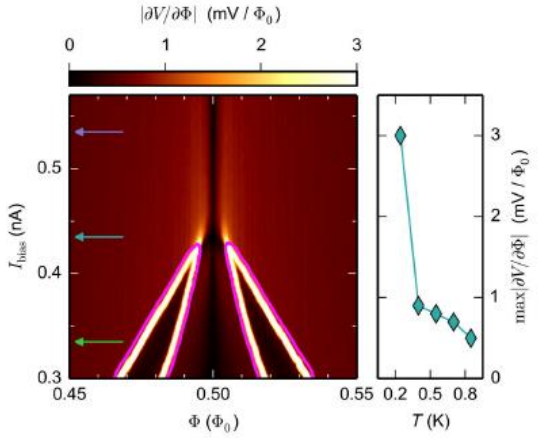

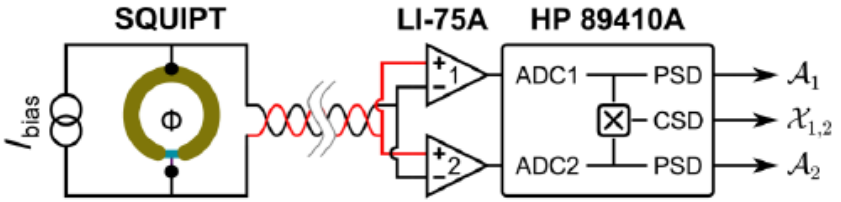

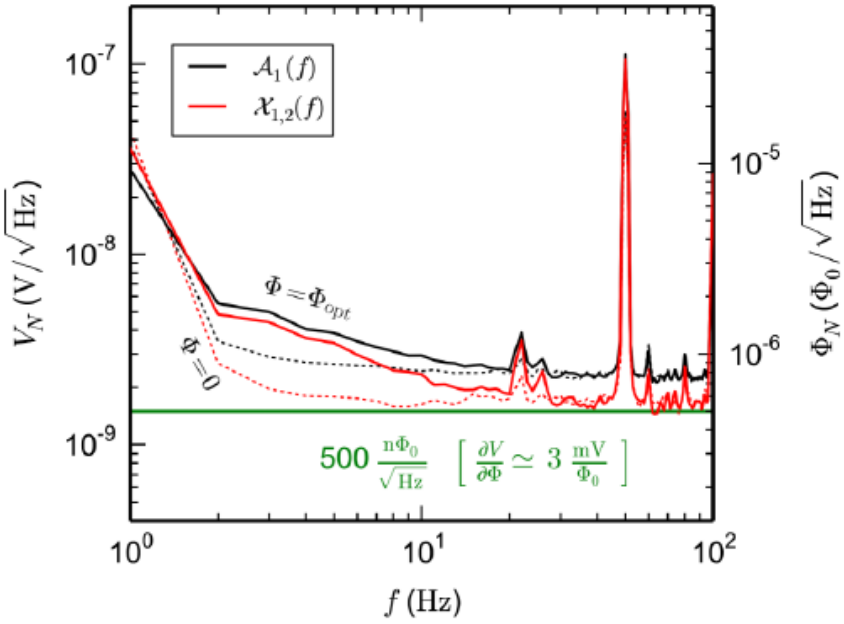

$$\Phi_N = \frac{V_N}{|\partial V/\partial\Phi|} \simeq 500 n\Phi_0/\sqrt{Hz}$$

FG *et al.*, Nat. Phys. **6**, 254 (2010);
M. Meschke et al., PRB **84**, 214514 (2011);
A. Ronzani et al., PRAppl. **2**, 024005 (2014);
S. D'Ambrosio et al., APL **107**, 113110 (2015)

The ω-SQUIPT: towards Josephson topological materials

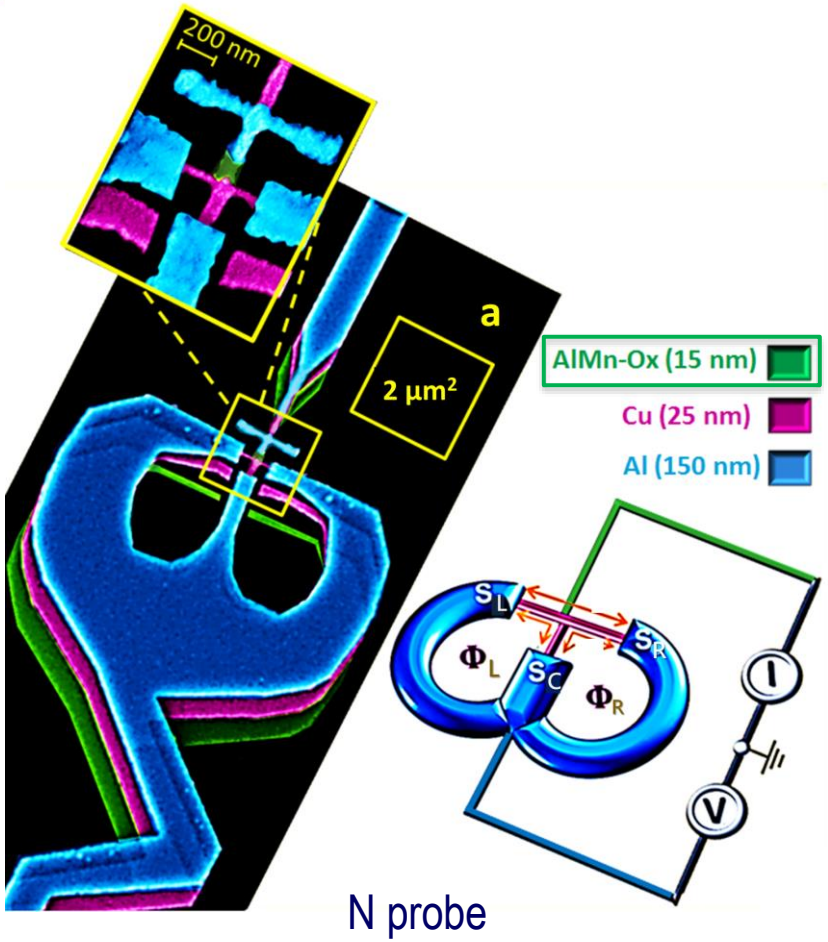

$$G(V,\Phi_L,\Phi_R) = \frac{1}{eR_T}\int_{-\infty}^{\infty} dE\ \ DoS(E)\ (-\frac{\partial f}{\partial E}(E-eV))$$

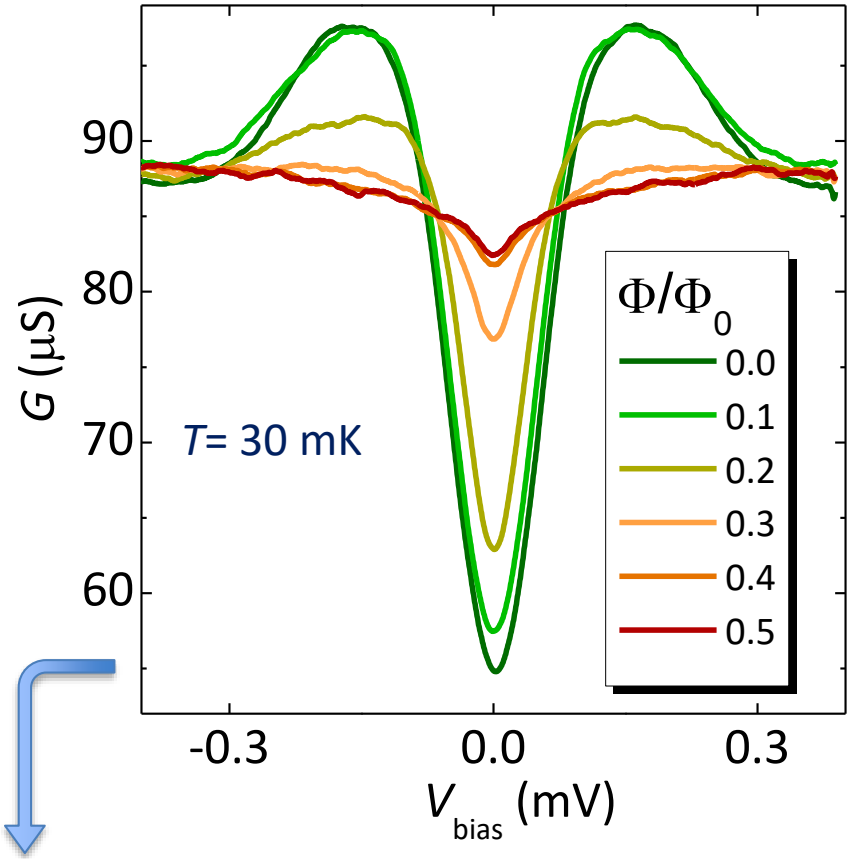

Picture *only* apparently similar to 2-terminal interferometer

The ω-SQUIPT (A-type – 30 mK)

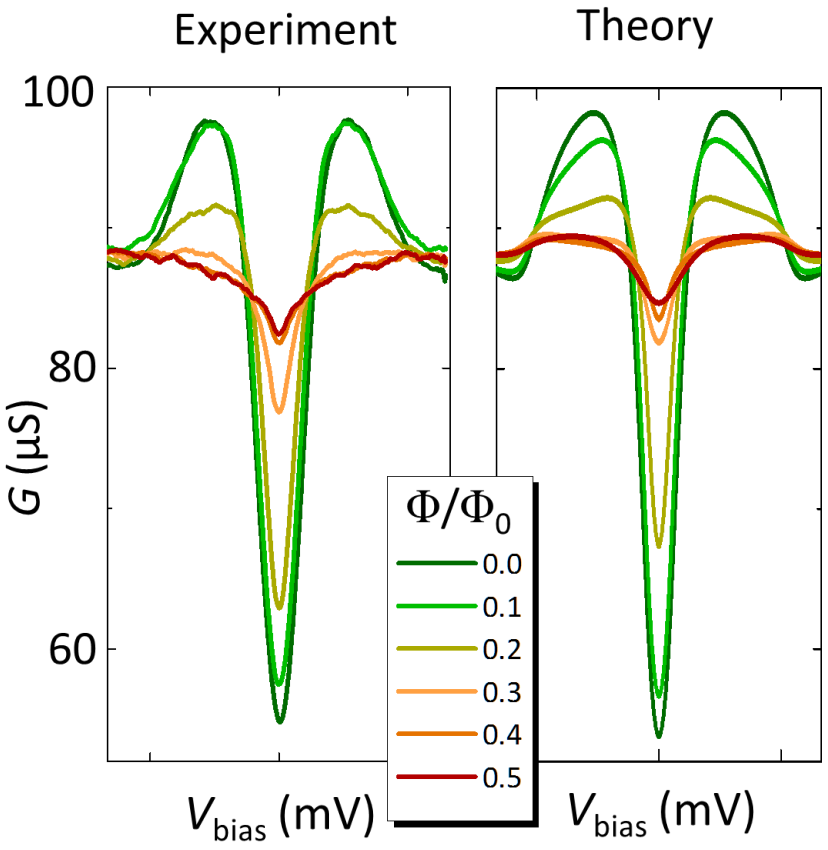

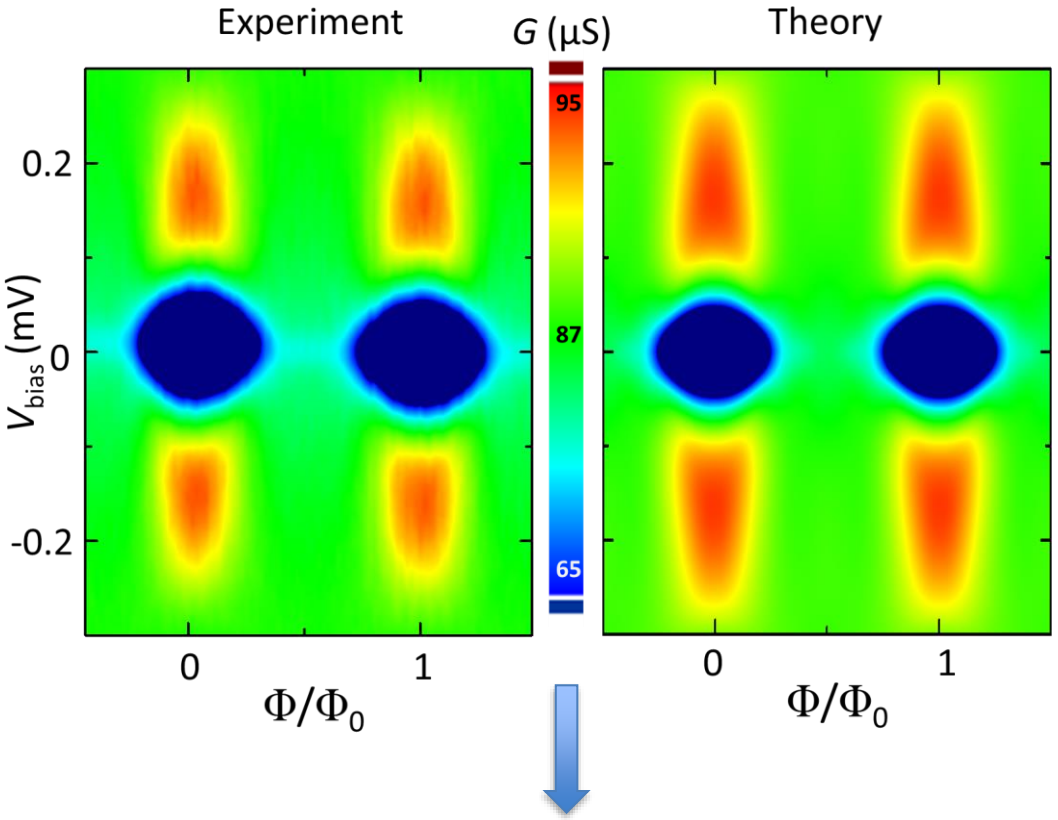

$R_T \approx 6.5\ \mathrm{k}\Omega$

$\Phi = \Phi_L = \Phi_R$

Presence of a minigap for $|\Phi/\Phi_0| \leq 1/4$

&

Gapless regime for $\Phi_0/4 \leq \Phi \leq 3/4\Phi_0$

E. Strambini, S. D'Ambrosio, F. Vischi, F. S. Bergeret, Yu. V. Nazarov, and FG, Nature Nanotech. **11**, 1055 (2016)

The ω-SQUIPT (B-type – 30 mK)

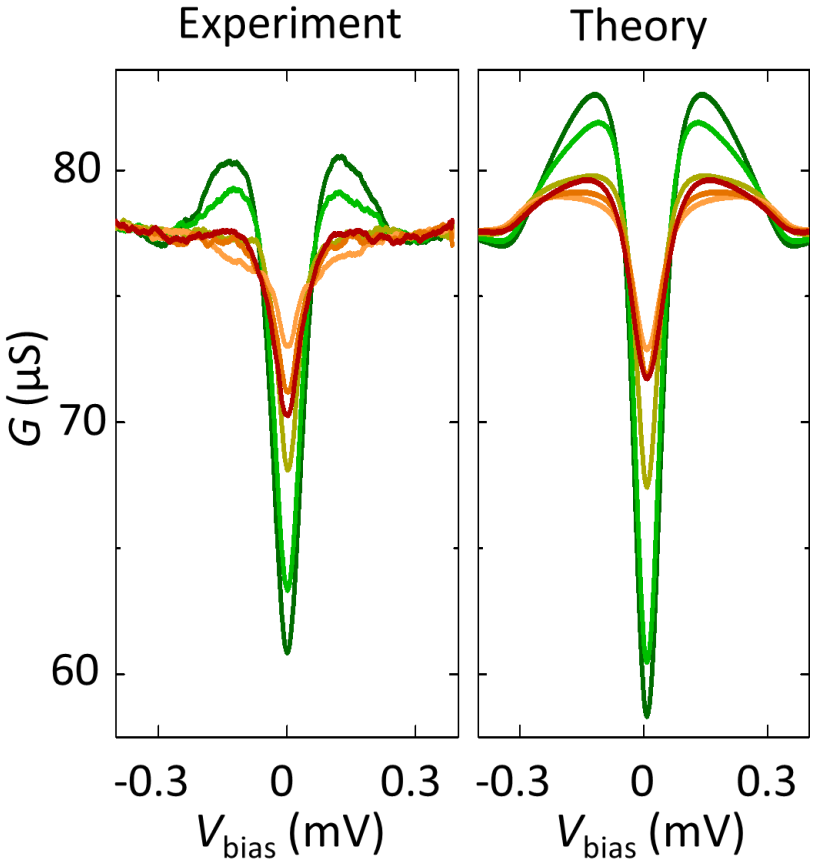

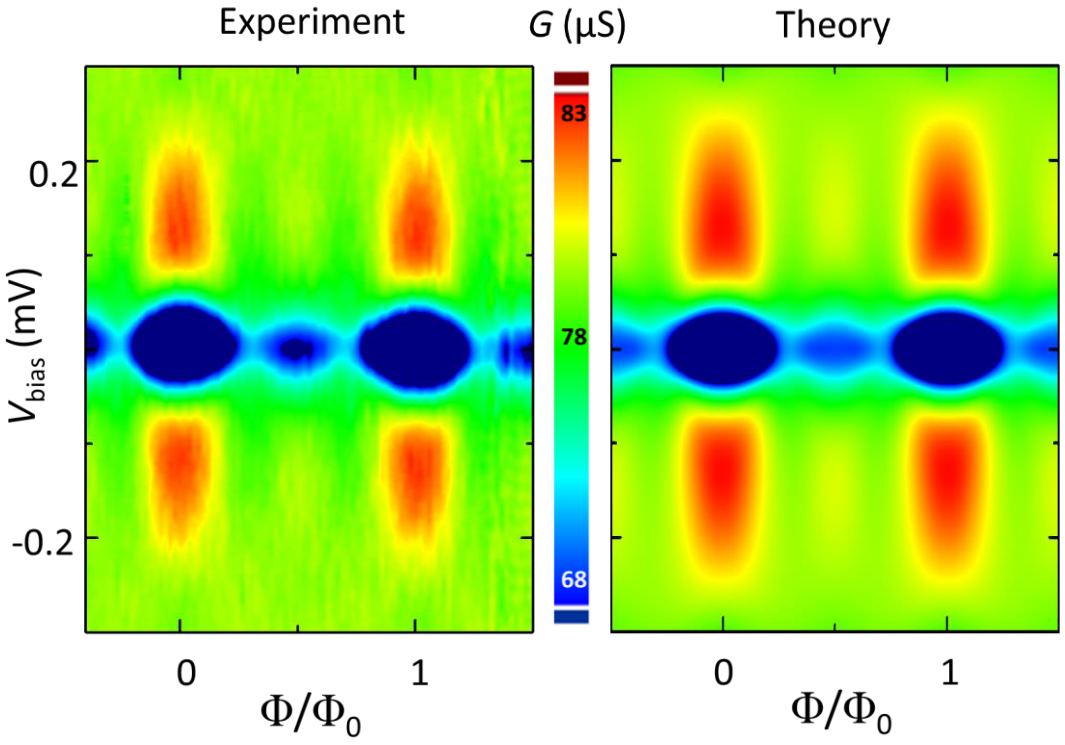

Presence of a second smaller minigap for $\Phi_0/4 \leq \Phi \leq 3/4\Phi_0$

$R_T \approx 8\ \mathrm{k}\Omega$

$\Phi = \Phi_L = \Phi_R$

E. Strambini, S. D'Ambrosio, F. Vischi, F. S. Bergeret, Yu. V. Nazarov, and FG, Nature Nanotech. **11**, 1055 (2016)

The ω-SQUIPT: topological classification

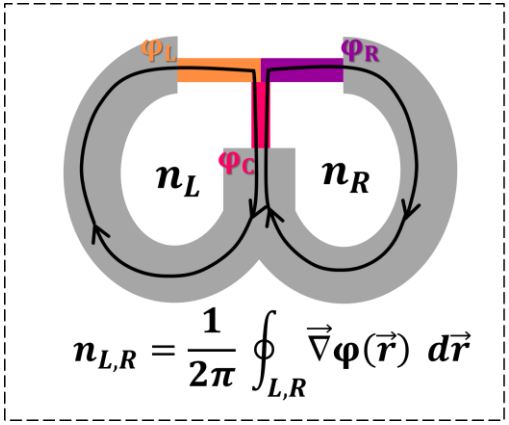

A-type

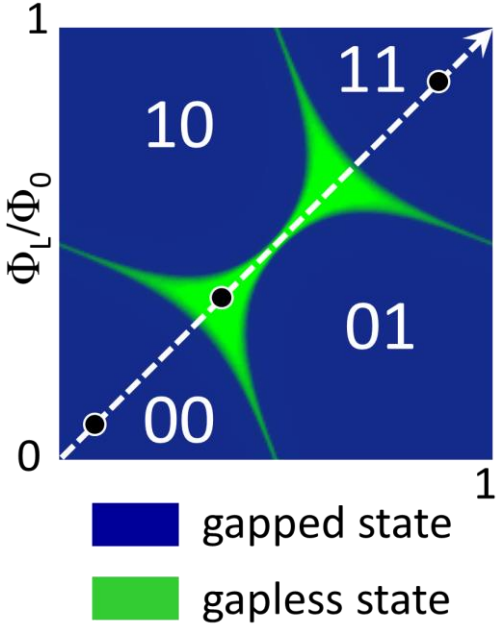

North pole – N state

Weak-link in a gapped state

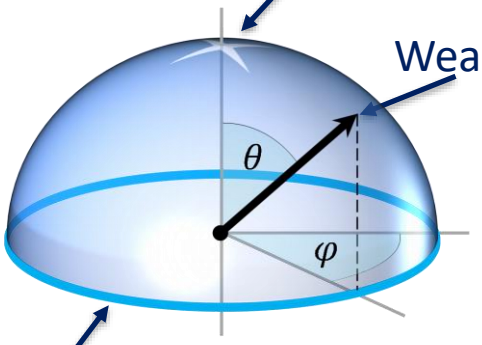

Equator – S state

θ - degree of superconductivity

φ - superconducting phase

B-type

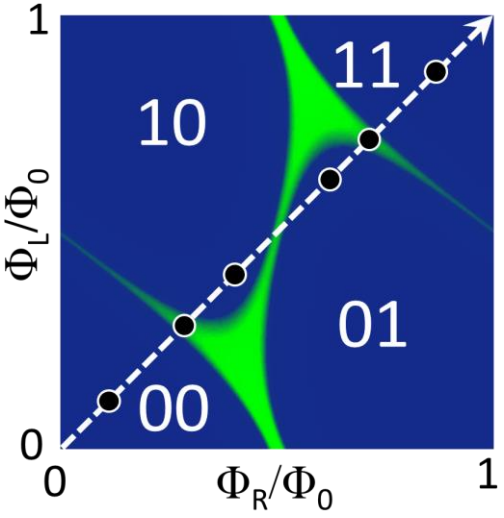

E. Strambini, S. D'Ambrosio, F. Vischi, F. S. Bergeret, Yu. V. Nazarov, and FG, Nature Nanotech. **11**, 1055 (2016)

C. Padurariu *et al.*, PRB 92, 205409 (2015)

The ω-SQUIPT: topological protection

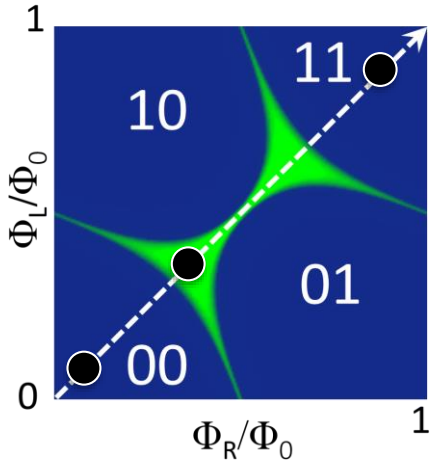

gapped state

gapless state

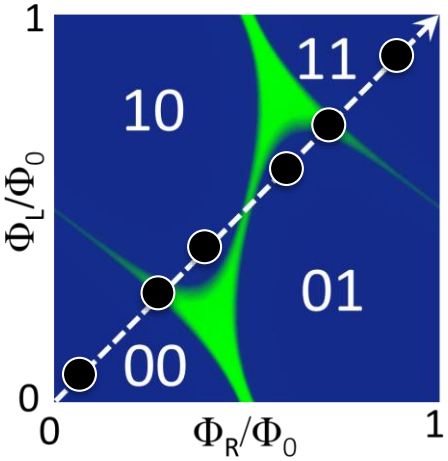

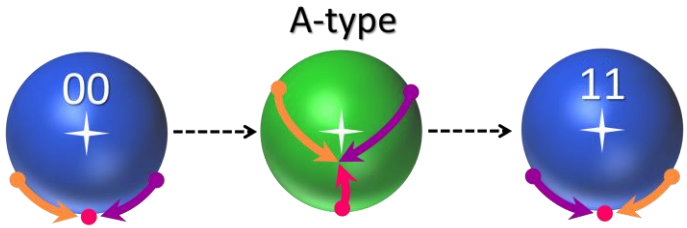

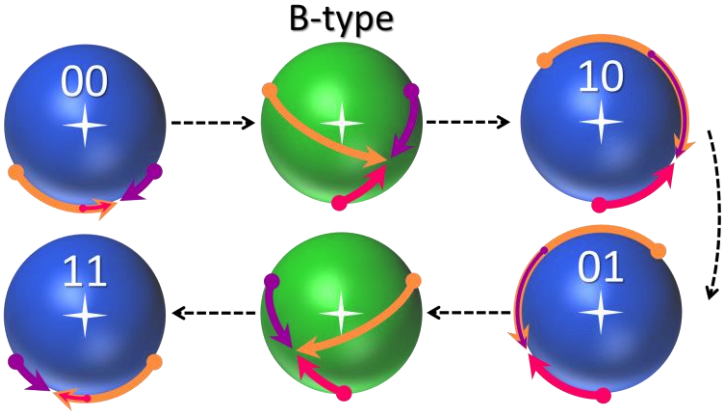

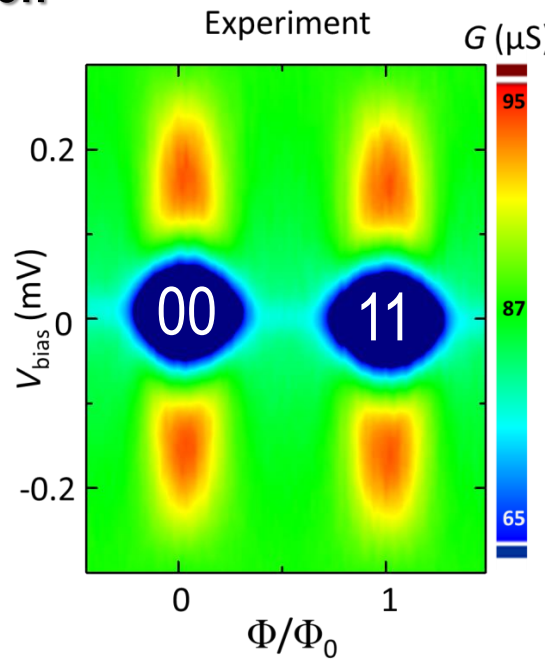

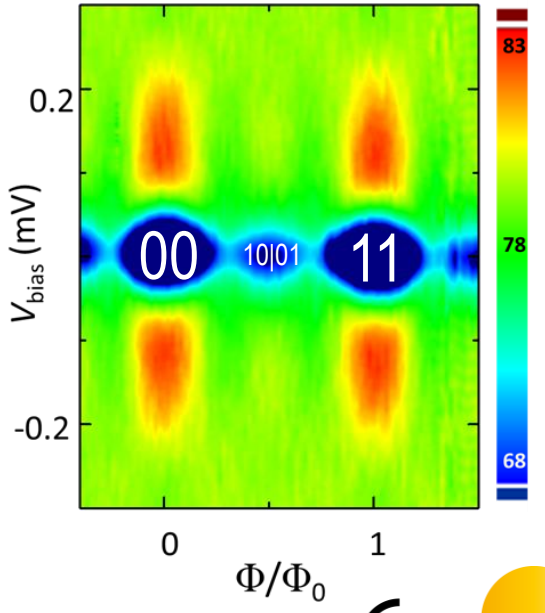

E. Strambini, S. D'Ambrosio, F. Vischi, F. S. Bergeret, Yu. V. Nazarov, and FG, Nature Nanotech. **11**, 1055 (2016)

The ω-SQUIPT: comparison with 2-terminal system

A-type ω-SQUIPT

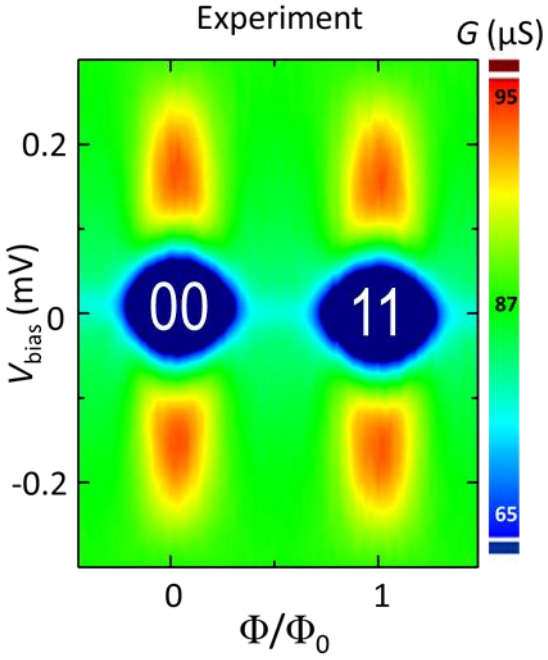

- Existence of a gapless state in a finite region of phases
- Switching between gapped and gappless states with a fine tuning of the phase
- The continuous gapless state demonstrates breaking of TRS expected in multiterminal (N > 2) geometries

B-type ω-SQUIPT

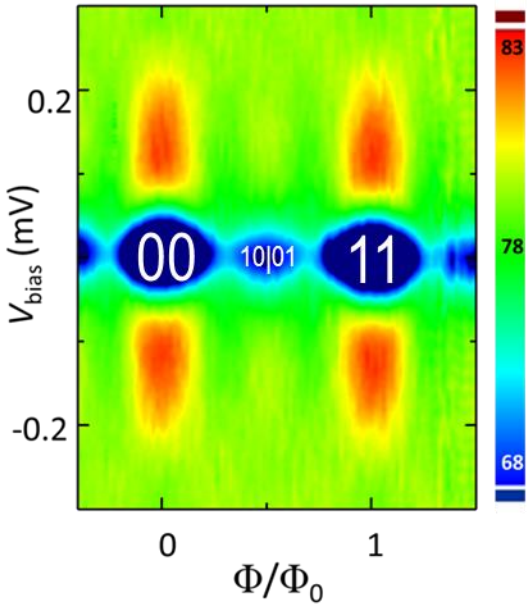

2-terminal SQUIPT

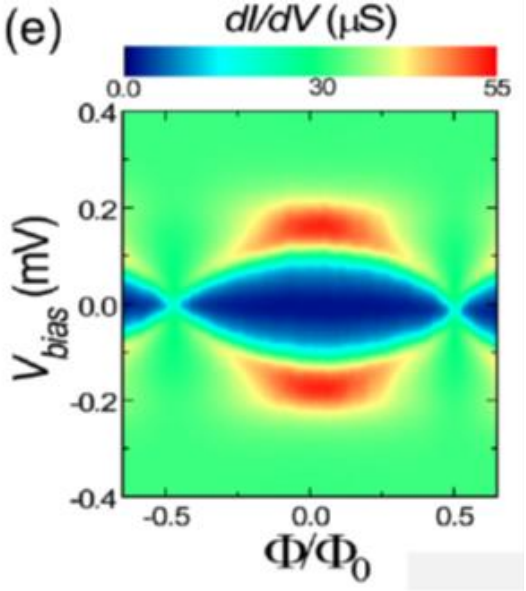

E. Strambini, S. D'Ambrosio, F. Vischi, F. S. Bergeret, Yu. V. Nazarov, and FG, Nature Nanotech. **11**, 1055 (2016)
C. Padurariu *et al.*, PRB **92**, 205409 (2015)

The ω-SQUIPT: nonlocal character of topology

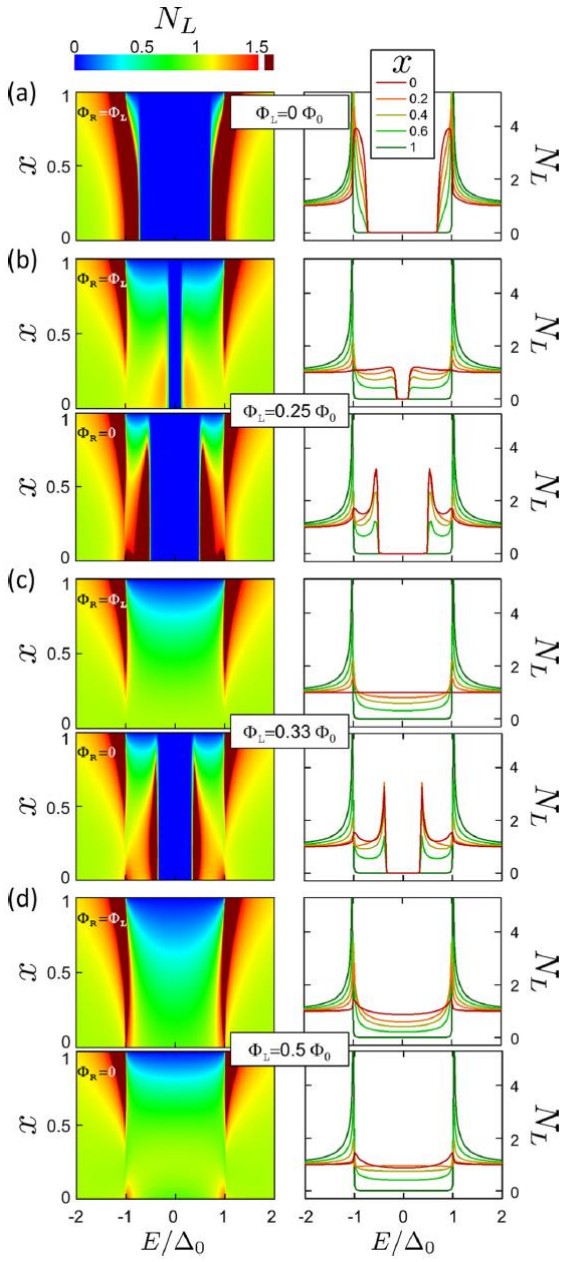

Gapped or gapless region is a nonlocal property of WL

F. Vischi *et al.*, Phys. Rev. B **95**, 054504 (2017)

The ω-SQUIPT: DoSs behavior vs junction length

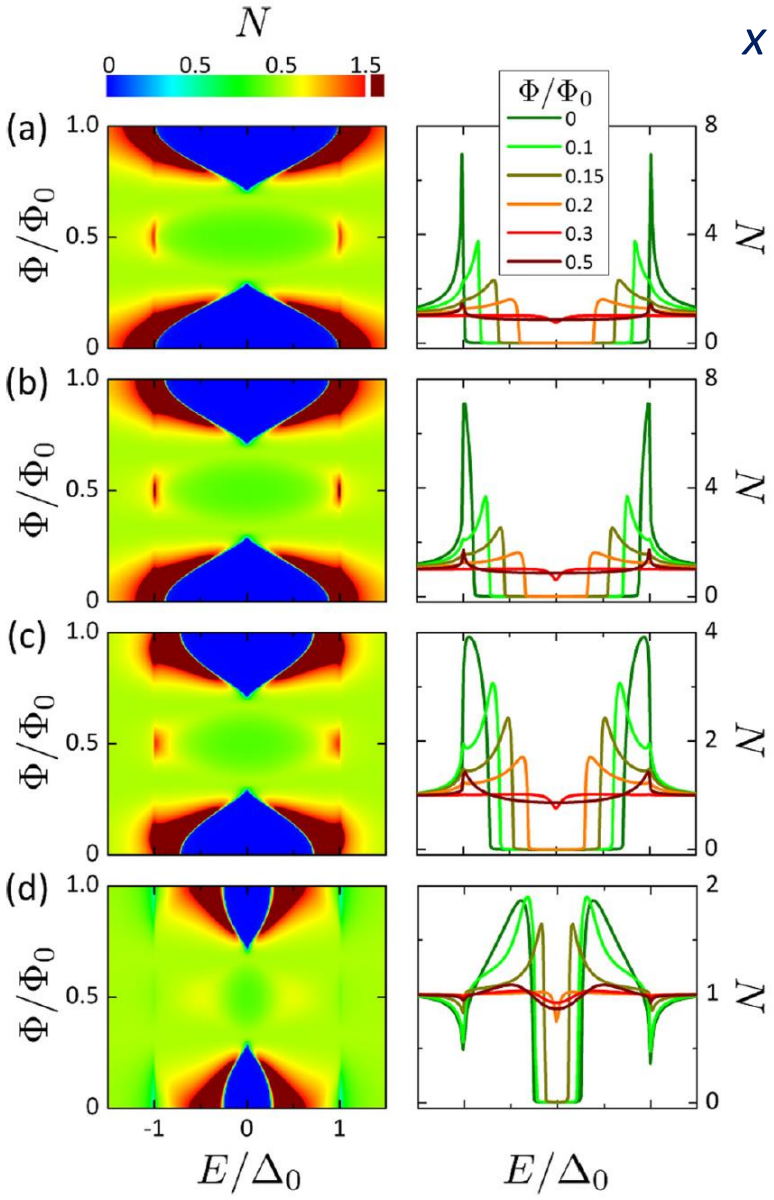

$x = 0$

Longer junction

Continuous gapless state

Main hallmark of multiterminal JJs

Crossing of ABS at zero energy

F. Vischi *et al.*, Phys. Rev. B **95**, 054504 (2017);
C. Padurariu *et al.*, Phys. Rev. B **92**, 205409 (2015)

The ω-SQUIPT: temperature dependence of topological transitions

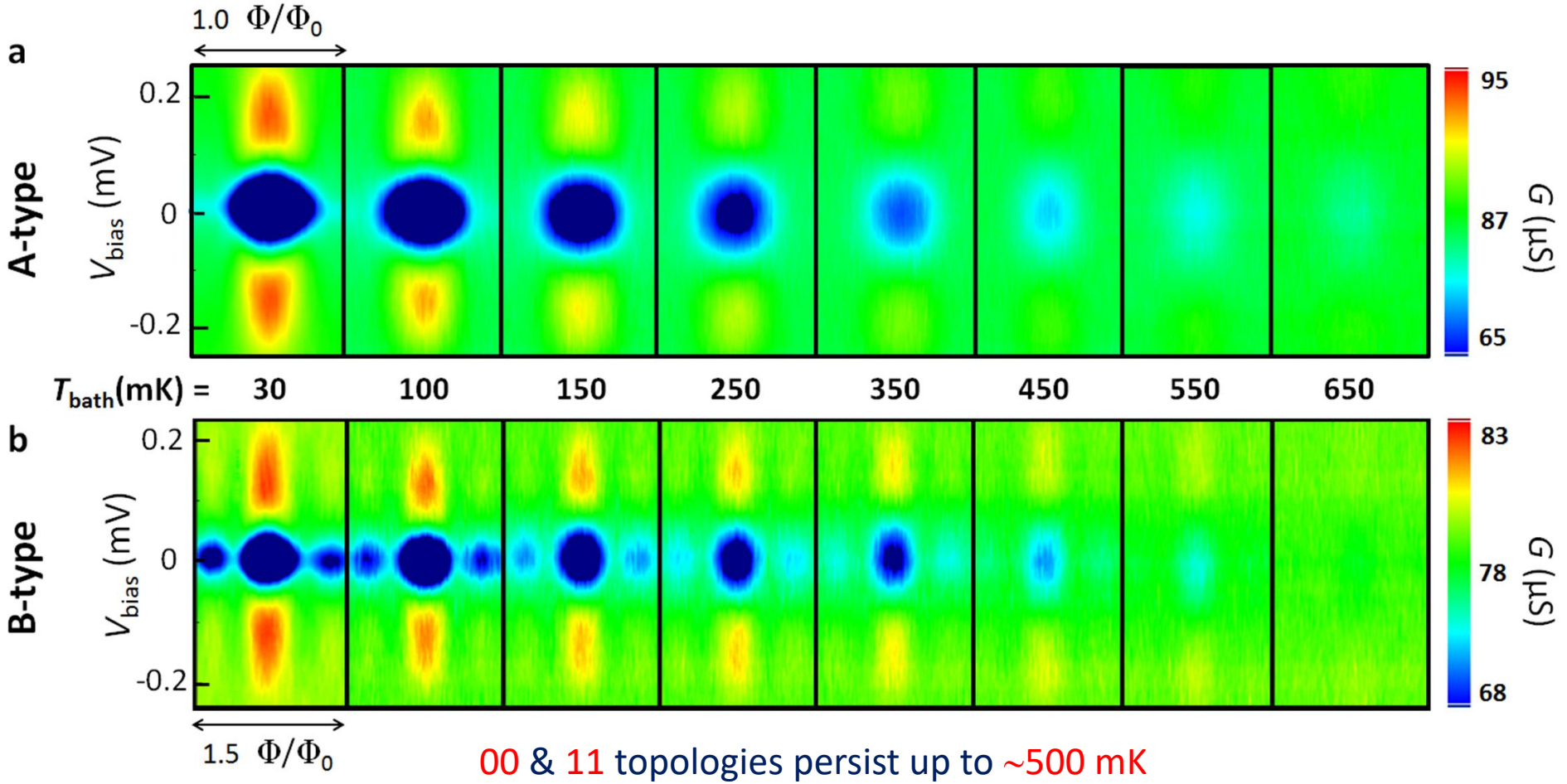

00 & 11 topologies persist up to ~500 mK

10 & 01 topologies persist up to ~300 mK

Higher T ⟹ larger E_{Th} and Δ

E. Strambini, S. D'Ambrosio, F. Vischi, F. S. Bergeret, Yu. V. Nazarov, and FG, Nature Nanotech. **11**, 1055 (2016)

Conclusions & future perspectives

1. Realization of the first double-loop SQUIPT with 3 S terminals
2. Enable exotic phase-engineering of the WL topology
3. Presence of gapped-like and gapless states, tunable with the magnetic field
4. The gapped-like states realize a 2D Josephson topological material univocally classified by (n_R, n_L)
5. Φ_0-periodic topological protected transition occurs over a continuous magnetic field interval (*symmetric* case)
6. Presence of 2 additional topologies in *asymmetric* interferometers
7. Continuous gapless-like state demonstrates TRS breaking expected for multi-terminal geometries
8. Pivotal constraint to access exotic topologies where individual ABS could be resolved
9. More S terminals will increase the phase dimensionality, enabling artificial topologies in an *hyperspace*
10. These topologically-protected states could allow the implementation of coupled flux q-bits, providing their interaction and entaglement

E. Strambini, S. D'Ambrosio, F. Vischi, F. S. Bergeret, Yu. V. Nazarov, and FG, Nature Nanotech. **11**, 1055 (2016);
F. Vischi *et al.*, Phys. Rev. B **95**, 054504 (2017)

Collaboration

E. Strambini, S. D'Ambrosio, F. Vischi, M. Carrega
NEST, Istituto Nanoscienze-CNR & Scuola Normale Superiore, Pisa, Italy

F. S. Bergeret
CFM-MPC, CSIC-UPV/EHU, San Sebastian, Spain

Yu. V. Nazarov
Kavli Institut of Nanoscience, Delft University of Technology, Delft, The Netherlands

Acknowledgement: ERC consolidator grant No. 615187-COMANCHE